

IMPROVED SEISMIC ASSESSMENT OF EXISTING RC FRAME STRUCTURES

Aleksandar Zhurovski ⁽¹⁾, Borjan Petreski ⁽²⁾, Igor Gjorgjiev ⁽³⁾

⁽¹⁾ Asst. Prof., Ss. Cyril and Methodius University in Skopje, Institute of Earthquake Engineering and Engineering Seismology (IZIS), Skopje, N. Macedonia, zurovski@iziis.ukim.edu.mk

⁽²⁾ Asst. Prof., Ss. Cyril and Methodius University in Skopje, Institute of Earthquake Engineering and Engineering Seismology (IZIS), Skopje, N. Macedonia, borjan@iziis.ukim.edu.mk

⁽³⁾ Prof., Ss. Cyril and Methodius University in Skopje, Institute of Earthquake Engineering and Engineering Seismology (IZIS), Skopje, N. Macedonia, igorg@iziis.ukim.edu.mk

Abstract

The seismic performance of building structures is governed by the lateral stiffness which is provided by the geometrical and material characteristics of their structural elements and their arrangement in plan and elevation. In general, the procedure for designing the structures to withstand the code-prescribed lateral loads is quite straightforward. However, the performance of the building subjected to realistic seismic loading is also important beyond the deterministically defined safety points that ensure life-safety at fixed return periods. Building structures in North Macedonia are designed according to an outdated code that does not consider the modern developments in the field of performance-based earthquake engineering such as ductility of the cross-section. Thus, the ratio of the column dimensions is not a matter of consideration when designing a structure and the weak beam – strong column concept is ignored in the designer's check list. Therefore, because of the need for open architectural spaces and aligned interior walls and columns, the designers often rotate the shorter cross-section dimension along the longer beam span. With the aim of investigating the effect of the orientation of the columns in plan on the seismic performance of reinforced concrete frame structures, an existing residential building is analyzed. The existing structure is compared with alternatively designed structural models with different column cross-sections or different orientation of the existing column cross-section in plan. The comparison is performed using nonlinear analysis of the existing structures and the proposed models. Then, a simplified probabilistic assessment of the structural configurations is performed, and the results are presented. Finally, the results are used to stress the need for assessment of the existing structures with the modern approaches employed in the more up-to-date design codes and performance-based earthquake engineering principles.

Keywords Seismic Assessment; RC frame structures; PERFORM 3D; probabilistic estimation.

1. Introduction

North Macedonia is located in the central part of the Balkan Peninsula, a region often in the history exposed by the devastating nature of strong earthquakes [1]. Therefore, the whole territory of the country is seismically active and intensity VII-IX earthquakes according to European intensity scale frequently occur. In the recent past, there have been several earthquakes that resulted in significant economic damage and social disruption. The most significant of them happened in 1963, when a 6.1 magnitude earthquake killed over 1000 people. After that earthquake, great effort was made in order to develop the building practice and improve the building stock in the country and in Europe in general. The building stock of North Macedonia is generally characterized by 2 types of buildings. The first type incorporates the buildings that were built prior to 1969 when the first seismic building code was implemented. These buildings do not meet the current seismic design standards and only a few of them are designed to resist lateral loads such as wind. The second type contains the structures designed to resist seismic forces, following the code from 1969 and the revised and more refined code from 1981. The newly built structures are also part of this type since the last revision of the seismic code is dating back to 1981.

Given that the structural response under earthquake loading is essential for structure's seismic resilience, especially beyond safety point defined by the code, it is crucial to design each structural element properly. Unfortunately, North Macedonia is one of the last European countries that uses outdated codes for seismic design of structures. Even though the 1981 code provides considerably good guidelines for design of earthquake resistant structures, it is based on general interpretation of the good seismic design practices and does not give details of the design details. Since the code has not been modified for a long time, it does not contain the state-of-the-art advancements in the earthquake engineering field such as the ductile capacity design. For example, in the current seismic code there are no strict guidelines for following the “strong column / weak beam” principle such as the capacity design guidelines in Eurocode 8 (EC8), CEN (2005) [2], apart from a recommendation that the formation of plastic hinges in the columns and joints should be avoided.

The architectural demand for open space very often implies the design of rectangular columns with small dimensions fully incorporated within the width of the infill wall (usually 25cm). Additionally, in some plan arrangements, the smaller side of the rectangular cross-section is oriented along a longer span. This results in a very small column capacity in the smaller side direction whereas the beam possesses greater dimensions and capacity to satisfy the span to depth ratio. Consequently, the smaller column capacity affects the global structural response under earthquake excitation.

To investigate the influence of the ratio of section sides of rectangular columns on the seismic performance of structures, an existing reinforced concrete (RC) frame structure designed according to Macedonian codes of practice was selected for analysis. The analyzed structure is a three-story residential building regular in plan and elevation. Nonlinear static pushover (SPO) analysis was performed on the existing structural configuration and its performance was evaluated through a SPO curve. The characteristic values regarding the current seismic code limits were plotted on the performance curve and the structural design was assessed. Then, additional three structural configurations were examined to demonstrate the performance differences between the structure designed with the current seismic code and the alternative configurations. Initially, the SPO response of the four models was investigated and compared. Due to the need to compare the response of the models for higher levels of nonlinearity, up to collapse of the structure, an improved procedure involving effective tool for estimating structure-specific seismic fragility curves was employed. Finally, the models were investigated for several performance levels and the performance differences were discussed.

2. Nonlinear Static Analysis Approach

2.1. Structural description of the building

The residential building being investigated is a three-story RC frame structure with story height of 2.9m. To achieve greater open space and flat interior walls, the columns were made rectangular. The building's plan shape is rectangular and can be classified as regular, as shown in Figure 1. The spans in x-direction measure 6.4m and 5.65m, while the spans in y-direction measure 3.4m and 4.5m. The beams are rectangular with dimensions of 25/40cm and 25/45cm, while all columns have dimensions of 25/45cm.

The structural design of the building is performed using the current Macedonian seismic code dating back to 1981. The loads are applied using the current codes of practice as well and their values are 1.50kN/m² dead load and 1.50kN/m² live load for residential areas. The snow load is applied on the third floor and it is taken as 0.75kN/m². According to the seismic code, the masses for calculation of the modal parameters and seismic forces are taken with coefficient 1.0 for dead load and snow load, while the coefficient for the live load is 0.5. Therefore, the floors' masses are 136t, 115t and 83t for the first, second and third floor accordingly. After the definition of masses, modal analysis is performed and translational modes in both principal directions are obtained. The first period in x-direction is 0.37s, while the first period in y-direction is 0.33s. The structure is located in zone IX of the seismicity zonation according to the European intensity scale and the seismicity coefficient for the calculation of base shear force is 0.1. Consequently, the total base shear force for the structure in x and y-directions is 335kN.

The effect of column cross-section orientation on the seismic response of the structure was investigated using four structural analytical models. In Model 1, the shorter section side of all columns is oriented along y-direction (C1 - 45/25 cm), while in Model 2, the shorter section side of all columns is oriented along x-direction (C2 - 25/45 cm). In the third analytical model, columns C1 and C2 are arranged in a mixed arrangement as it was originally designed. The need for the layout of the structure in Figure 1 is a result of architectural demands. Thus, there are columns that are oriented with shorter section sides along the longer span. The last model, Model 4, is a structure that has a square cross-section of all columns (C4 - 35x35cm), which the authors consider the most suitable column cross-section for such a building providing equal resistance in both directions.

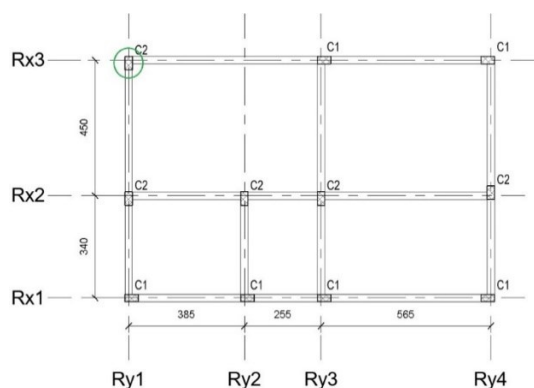


Figure 1. Characteristic floor plan of the example building (Model 3).

2.2. Numerical modelling

The SPO analysis was performed using the Perform3D software for nonlinear analysis and design [3]. Depending on the modelling requirements, there are several different types of elements available for use. Each element consists of numerous basic components that are used to simulate the nonlinear behaviour of all types of structural elements. For this case study, the basic components used for the modelling are as follows:

- Inelastic non-buckling steel material was defined for the reinforcement according to the provisions given in the national standard. The stress-strain relationship of the reinforcement was modelled as trilinear, with strength loss (at point L), without cyclic stiffness degradation. The model curve is shown in Figure 2 (left).
- A macro model with Mander stress-strain relationship is most frequently used to describe the working condition of confined concrete in uniaxial compression [4], which is related to section shape and the configuration condition of the stirrup. By the program, the model is transferred in the standard force-deformation (F-D) relationship. Hence, for the design quality of concrete, a concrete model curve was computed according to the Mander model, mean value of concrete's strength and elastic modulus (Figure 2 - right).

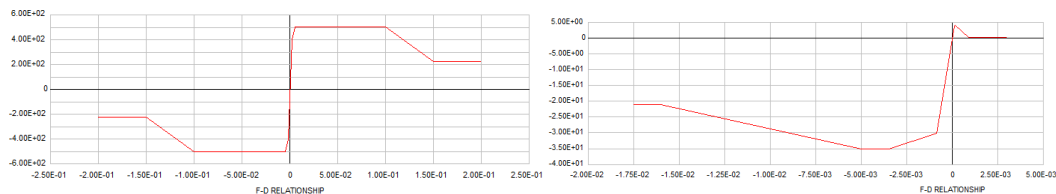


Figure 2. Material models for reinforcement (left) and confined concrete (right) from Perform3D, Computers and Structures, Inc. (2018).

The properties of steel material are defined by a yield strength of $f_y=400\text{MPa}$, a yield strain of $\epsilon_y=2\%$, an ultimate strength of $f_u=500\text{MPa}$ and an ultimate strain of $\epsilon_u=25\%$. The Mander stress-strain model for confined concrete is used to determine the properties of the concrete material. Hence, the typical values are $f_{co}'=30\text{MPa}$, $f_{cc}'=35\text{MPa}$, $\epsilon_{co}=2\%$, $\epsilon_{co}=3.5\%$ and $\epsilon_{cu}=17.5\%$ (the ultimate compressive strain ϵ_{cu} is obtained at first hoop fracture).

Inelastic fiber sections were used for modelling of the columns. They were assigned at the corresponding lengths of the elements to simulate the plastic hinge region, with the rest of the element remaining elastic. The beams were modelled following the lumped plasticity approach using inelastic rotational moment hinges. The joints were considered as fully rigid and they were modelled using rigid elements.

2.3. Analysis procedure

The use of nonlinear static analyses has been increasing recently, in contrast to ductility-modified spectra analyses. Nonlinear static analysis, also known as pushover analysis, accurately defines the deformation curve of a structure and demonstrates its capacity through a pushover curve. This method is considered a step forward from the use of linear analysis and ductility-modified response spectra because it is based on a more accurate estimate of the distributed yielding within a structure, rather than an assumed, uniform ductility [5]. Nonlinear response analysis is performed for many reasons, including the design of new buildings and assessing the performance of existing and new buildings, as per the NEHRP classification [6]. Furthermore, a number of codes and guidelines have designated it as the preferred assessment procedure [7].

The performance of the investigated structural configurations was evaluated through static pushover analyses. A predefined set of lateral forces was applied to the structures stepwise, based on their masses and first mode shape vectors. The stiffness matrices were updated at each step of the analyses to account for the yielding of beams or columns. The pushover analyses were executed until the structures collapsed.

Because of the outdated Macedonian seismic design code, the performance levels for the assessment of structures were obtained from more advanced contemporary codes of practice. As an example, the Italian National Code defines 4 limit states: Operational, Damage Control, Life Safety and Collapse Prevention [8]. Based on FEMA 273 recommendations [9], [10], [11], for concrete frames, drift limit indicators are provided following the structure's response to different performance levels. FEMA 273 categorizes the drift limitations in three classes: 1) immediate occupancy, represented with 1% transient

and negligible residual drift, 2) life-safety, exhibiting maximum of 2% transient and 1% residual drifts, and 3) collapse prevention, limited with 4% of transient and residual drifts. Therefore, in this study, a combination of the codes of practice can be observed as the FEMA 273 performance assessment limits are used for concrete frames designed following the Macedonian code of practice.

The deformation capacities for the components or the so-called performance acceptance criteria corresponding to different building performance levels were defined in terms of plastic rotation capacities. In the present study, plastic rotation capacities for Immediate Occupancy (IO), Life Safety (LS) and Collapse Prevention (CP) levels were used for the column and beam elements (Table 1). In the analysis, only one criterium was used for performance-based evaluation. Namely, the performance of the structure was evaluated based on the flexural behavior of the columns only. It was assumed that the flexural behavior of the columns governs the structure's behavior, and the columns define the structure's failure mechanism. For the analysis, the rotation capacities in columns were used as referent. The damaged state of the structure corresponded to reaching the specified level of rotation in columns.

Table 1. Rotation capacities and colour designation for the structural elements used in the analysis.

Performance Level	Column Rotation Capacities (rad)	Beam Rotation Capacities (rad)	Colour
IO	0.005	0.005	Cyan
LS	0.025	0.025	Yellow
CP	0.035	0.050	Red

2.4. Column cross-section ductility calculation

The moment-curvature relationships of a column section are very important to assess the ductility of the element, the amount of the possible redistribution of stresses and its resistance against dynamic loading. Calculation of the moment-curvature relationship of the three implemented column cross-sections was performed using the tool developed by Bentz and Collins [12]. Moment-curvature relationships of the column cross-sections were calculated along the local x-axis for columns C1(45x25cm), C2(25x45cm) and C3(35x35cm) for predefined axial force from the gravity loads (Figure 3). The reinforcement area in the column cross-sections is taken as 1% of the concrete section area, proportionally distributed along the section sides.

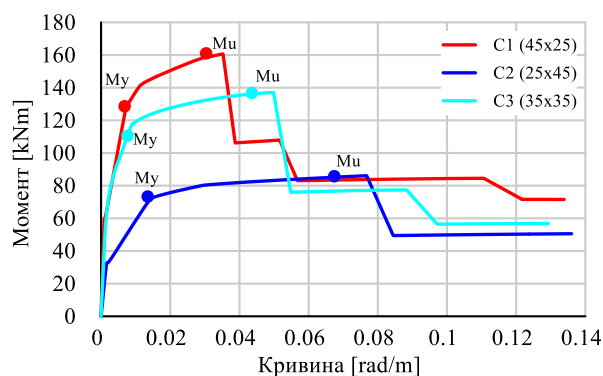


Figure 3. Moment-curvature relationships of the column cross-sections for gravity loads axial force.

Column C1 has the largest moment capacity, while column C2 has the lowest moment capacity, as observed in Figure 3. The yielding moment M_y for column C1 is 134kNm for C2 is 76kNm and for C3 is 112kNm. Column C1 has an ultimate moment M_u of 167kNm, column C2 has an ultimate moment M_u of 92kNm, and column C3 has an ultimate moment M_u of 141kNm.

Table 2 presents the calculated curvatures at yield and ultimate moments of the columns for three different levels of axial force. The curvature ductility of all concrete columns is calculated accordingly. It is defined as the ratio of ultimate curvature to yield curvature and it presents a metric for warning of

failure. C1 has a ductility of 5.05 for design gravity axial load, while C2 and C3 have a ductility of 6.73. The square column C3 exhibits a balanced behaviour in terms of ductility and moment capacity along both axes compared to the rectangular columns investigated. Two additional axial load levels are included in Table 2 to display the variations in axial load in the column due to the pushover analysis.

Table 2. Characteristic curvature and curvature ductility values for the investigated column cross-sections.

Column	N = 380kN			N = 300kN			N = 550kN		
	φ_y	φ_u	μ_φ	φ_y	φ_u	μ_φ	φ_y	φ_u	μ_φ
	[rad/m]	[rad/m]		[rad/m]	[rad/m]		[rad/m]	[rad/m]	
C1	0.00767	0.03878	5.05	0.00767	0.03525	4.59	0.00844	0.03878	4.59
C2	0.01141	0.07678	6.73	0.01141	0.07678	6.73	0.01256	0.07678	6.12
C3	0.00741	0.04986	6.73	0.00741	0.04986	6.73	0.00815	0.04986	6.12

2.5. Evaluation of the seismic performance

The results obtained from the nonlinear static analysis in terms of Pushover curves (Base shear vs. Top Drift) for the four models in both x and y orthogonal directions are shown in Figure 4. The diagrams display various top drift levels arranged in regions (cyan, orange, red). The lines that lie in these regions were set by following the response of the structure under the increasing displacement in the analysis and the nonlinear response of the columns, as they are governing the stability of the building structure. Table 1 rotation capacities are the basis for the acceptance criteria. Roof drifts when the structures reach IO, LS, and CP damage states (acceptance criteria) are designated in the figure.

Figure 4 shows that the base shear capacity is highly influenced by the column cross-section orientation in plan. Model 1 has the greatest base shear capacity in the x-direction (the direction of the longer column cross-section side), while Model 2 has the greatest base shear capacity in the y-direction. It is noted that the base shear capacity of Models 3 and 4 is similar and demonstrates uniformity in both directions. This is a demonstration of how a balanced choice of column cross-section orientation for Model 3 and a good choice of rectangular column cross-sections for Model 4 can be achieved. On the other hand, Models' 1 and 2 base shear capacity in both orthogonal directions shows differences of more than 30%.

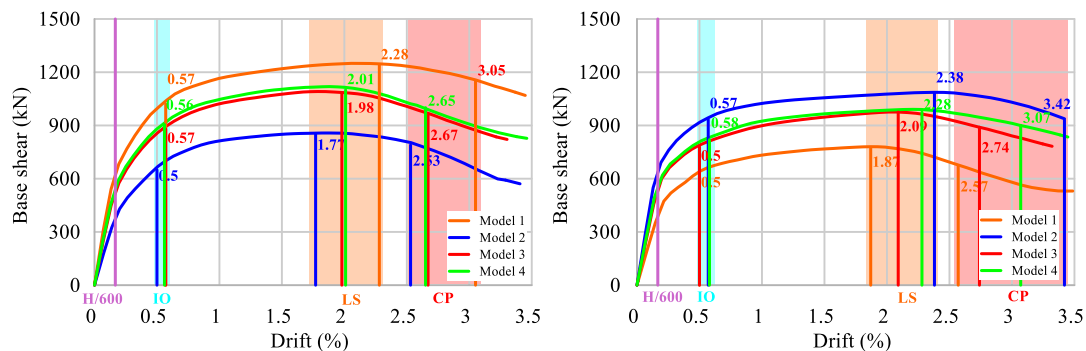


Figure 4. Pushover curves for Models 1, 2, 3 and 4 in x-direction (left) and y-direction (right).

Regarding the Macedonian code of practice and its total horizontal deflection limitations ($H/600$, where H is the total height of the structure), it is observed that the IO performance criteria are reached at greater drift level for every model. This demonstrates the stringency of the Macedonian seismic code of practice since the total drift limitation is at 1/3 of the earliest plastic rotation capacity of a column as per the IO performance criterium.

The design base shear is another parameter that has been investigated in accordance with the Macedonian seismic code. The structures are designed with a total base shear load of 335kN, for which the previously mentioned total drift limitation is assessed. This study demonstrates that the drift of the

lowest capacity models in each direction is closest to the $H/600$ limitation, while Models 3 and 4 exhibit lower drifts for the same base shear load.

The models' responses to the performance criteria levels vary as well. The IO performance level region is quite narrow, and the results for each model are similar, with the highest difference being 16%. On the other hand, the behaviour of the models in the LS and CP regions is more varied. The drift regions are wider and are associated with the plastic rotation capacities of the columns for LS and CP performance levels. Variation in global structural ductility of the models investigated is indicated by the difference in the width of the LS and CP regions and the narrowness of the IO performance level region. In the next chapter, the seismic response of the structural configurations is evaluated probabilistically for all performance levels, and this variance is investigated.

Figure 5 contains the damage state of the structure and the performance of the columns when the IO damage state is reached. It should be noted that the color when a column reaches a certain rotation capacity limit is given in table 1 and it corresponds to the colors given in the diagrams and figures.

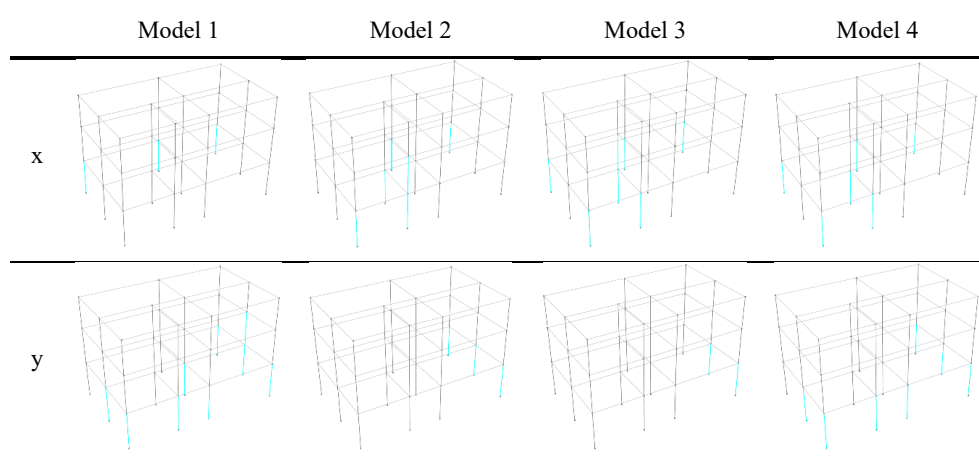


Figure 5. IO damage states in x and y-direction for Models 1, 2, 3 and 4.

The models investigated have some similarities, as shown in Figure 5. It was previously established that the response of the four models for IO performance level is similar. Thus, figure 5 additionally shows that IO is reached only for the ground floor columns for every model. However, the pattern for each model is different and governed by the column cross-section orientation and span length. The three-dimensional analysis additionally allows for different redistribution of loads for each model and affects the varying plastic rotation demand pattern.

3. Probabilistic Estimation of Seismic Response

When considering design of new structures or assessment of existing ones, the codes of practice usually provide limit values for deterministic assessment of structural performance. That is the only method available for design and assessment of structures subjected to earthquake loading, especially in more outdated seismic codes. The more up-to-date codes of practice provide the designers with some possibilities to choose probabilistic techniques for more realistic evaluation of the seismic response of the structural system. Since nothing is perfect and one needs to look at the problems probabilistically, especially in highly nonlinear behaviour where many uncertainties are involved, the probabilistic evaluation supplies seismic response evaluation in form of fragility functions.

Performance-based earthquake engineering (PBEE) is a structural engineering paradigm that fully embraces the intrinsic uncertainty associated with strong ground motion and employs probabilistic tools to evaluate structural performance in seismic areas [13]. The fragility functions are represented via a lognormal distribution that represents the probability of some 'failure', defined by a median η and dispersion β . They are usually derived from Incremental Dynamic Analysis (IDA) given in Vamvatsikos

and Cornell [14] or Multiple Stripe Analysis (MSA) which matches the building code intensity-based approach.

For the purpose of probabilistic evaluation of the seismic response of the structural configurations investigated, a simplified SPO-based procedure for estimating structure-specific seismic fragility curves of buildings is employed. The utilized SPO2FRAG tool simplifies the computationally demanding IDA by taking advantage of the SPO2IDA algorithm [15]. Basically, it accepts as input static pushover results obtained from the structural analysis software package of the user's choice and allows the user to control the IDA simulation and fragility estimation procedure at its various steps and intervene where one deems necessary [16]. The fragility function parameters are estimated as in Equation 1, where the terms $Sa_{f,x\%}^{LS}$ represent the x% fractile of the structural intensity causing exceedance of each limit state LS.

$$\begin{cases} \eta = \ln(Sa_{f,50\%}^{LS}) \\ \beta = \ln(Sa_{f,50\%}^{LS} / Sa_{f,16\%}^{LS}) \end{cases} \quad (1)$$

It is straightforwardly inferred from the above that such a simplified methodology for substituting a complex analytic procedure such as IDA involves many approximations and assumptions. Some of the basic assumptions for performing the simplified fragility curve calculation procedure include:

- As a consequence from IDA's intensity measure based (IM-based) fragility function development, the EDP random variable conditioned on the IM is independent of other ground motion features needed to evaluate the seismic hazard for the site, such as magnitude and source-to-site distance.
- Transformation from multi degree of freedom (MDoF) to single degree of freedom (SDoF) system with equivalent period of vibration T^* .
- A quadrilinear fit of the SDoF backbone curve according to De Luca et al. [17].
- Use of approximate equations for the lateral post-yield deformation profile suggested in FEMA P-58-1 (FEMA 2012) to convert the IDAs into interstorey drift ratio (IDR).

The simplified methodology for fragility curve estimation offers implementation of other sources of variability. Hence, the user is allowed to account for variability at nominal yield due to higher-mode effects and modelling uncertainty. According to Baltzopoulos et al. [16] there is a good agreement between the SPO2FRAG and analytically derived estimate of the fragility curves even without considering estimation uncertainty. Therefore, it is decided that for the sake of simplicity, there is no need for addition of variabilities for the investigated simple RC moment frame structures.

In order to be consistent with previous research and the examples provided by the developers of SPO2FRAG tool, the three-dimensional structure of this study is substituted with selected frames in both directions and turned into a two-dimensional problem. For the probabilistic estimation of seismic response, frames Rx3 and Ry1 of the structure are analyzed and SPO curves obtained. Figure 6 presents the SPO curves of the selected frames.

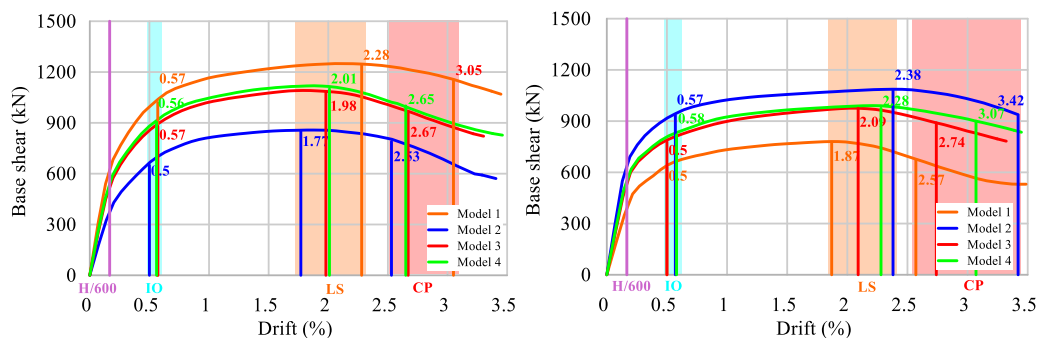


Figure 6. Pushover curves for selected frames from Models 1, 2, 3 and 4: frame Rx3 (left) and Ry1 (right).

Five performance levels for the development of structure-specific seismic fragility curves are defined by the user. The software tool incorporates the following limit states: fully operational (FO), immediate occupancy (IO), life safety (LS), collapse prevention (CP) and side-sway collapse (C). The FO limit state is set to 0.5% IDR while the C limit state is added by SPO2FRAG automatically when the quadrilinear fit of the backbone curve exhibits strength degradation in the form of a negative-stiffness branch. The other three performance levels (IO, LS and CP) are defined using the SPO curves and previous research studies. Results from the fragility curves development using the SPO2FRAG tool are given in Tables 3 and 4.

Table 3. Lognormal fragility function parameter estimates from SPO2FRAG – frame Rx3.

Limit state	Rx3							
	M1		M2		M3		M4	
	η (g)	β	η (g)	β	η (g)	β	η (g)	β
FO	0.283	0	0.161	0	0.259	0	0.246	0
IO	0.453	0	0.258	0	0.414	0	0.394	0
LS	1.128	0.157	0.670	0.156	1.038	0.173	0.992	0.155
CP	2.054	0.316	1.285	0.301	1.891	0.326	1.821	0.312
C	2.969	0.421	1.690	0.370	2.594	0.416	2.539	0.404

Table 4. Lognormal fragility function parameter estimates from SPO2FRAG – frame Ry1.

Limit state	Ry1							
	M1		M2		M3		M4	
	η (g)	β	η (g)	β	η (g)	β	η (g)	β
FO	0.418	0	0.625	0	0.584	0	0.553	0
IO	0.659	0.097	0.961	0.092	0.902	0.097	0.860	0.089
LS	1.428	0.311	1.978	0.303	1.875	0.308	1.800	0.301
CP	2.344	0.463	3.173	0.463	3.030	0.467	2.906	0.460
C	2.851	0.516	4.110	0.553	3.793	0.537	3.603	0.525

The results from the fragility estimation of the investigated models show consistent trends in several aspects regarding both frames, Figure 7. For the frame Rx3, the FO and IO results show similar values for the median value of the IM $S_a(T^*)$. The only difference is observed in Model 2 which shows significantly smaller values of exceedance for those performance levels. This is due to the orientation of the cross-section of the rectangular columns. When considering the ranges with considerable inelastic behaviour of the structures, the differences between the structural response of the model increases. However, Models 3 and 4 tend to present matching results even in these performance regions. Similar results have been observed for Ry1 as well. In this case study, Model 1 exhibits the exceedance of the structural demands at lower IM values. From this example it is clearly observed that the differences between the models are increasing as the nonlinearity of the problem increases. Regarding the comparison in the behaviour between both frames it is obvious that Ry1 shows better performance for all limit states and the reason for that is the lower tributary mass for that frame according to the structural configuration shown in Figure 1 and the smaller beam spans.

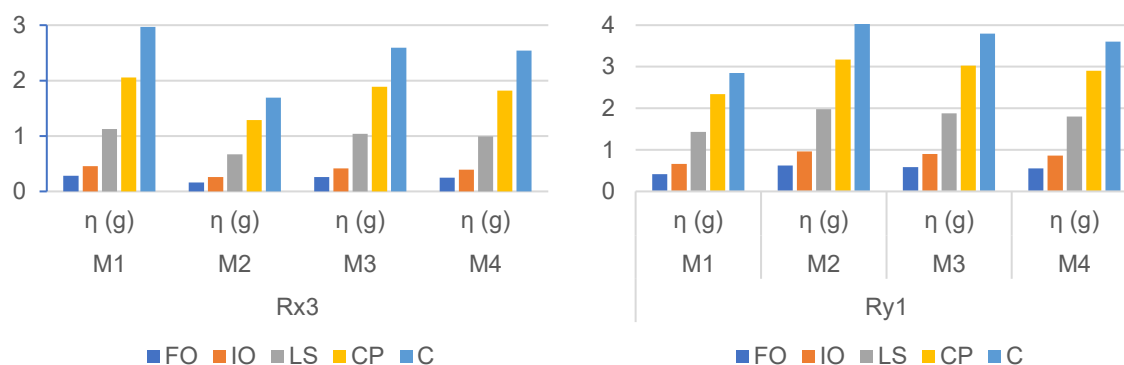


Figure 7. Median $S_a(T^*)$ intensities for each performance level for Rx3 (left) and Ry1 (right)

Another important point is the distribution of the dispersion values among the different limit states, which is an indicator of the IM efficiency. This distribution is shown in Figure 8. From Figure 8, one can observe the similarity of dispersion values for the LS limit state across all models. This suggests that $S_a(T^*)$ is a solid indicator of structural response for structures responding in their linear elastic range. Additionally, one can also observe the absence of dispersion values for FO and IO performance levels for Rx3 and only FO for Ry1. This shows the uniformness of the responses in the linear region of the structures. However, when considering highly nonlinear response of the frames, the dispersion increases. Comparing these dispersion values to some existing values in the literature, the values appear reasonable and of the same order of magnitude, with FEMA P695, FEMA (2009), proposing values of β between 0.10 and 0.50 depending on how well the model represents the actual structural behaviour and how robust that numerical model is O'Reilly and Sullivan (2018).

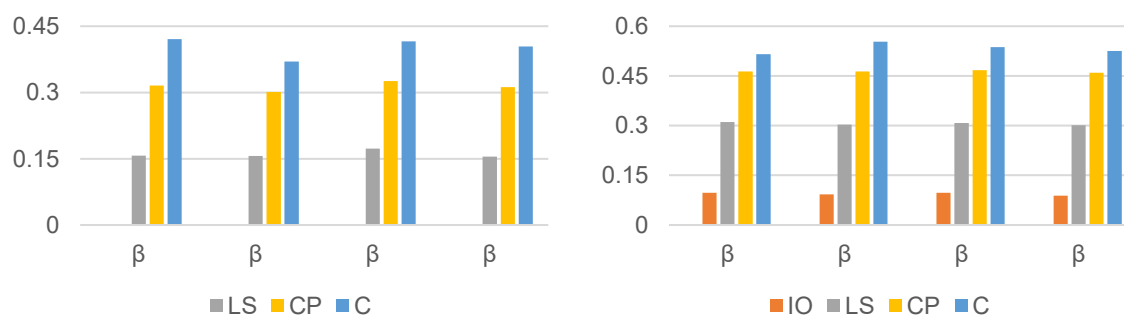


Figure 8. Dispersion values for each performance level for Rx3 (left) and Ry1 (right)

4. Conclusion

This study depicted a comparison arising from an ongoing problem in the structural engineering field. A number of cases were examined using a more sophisticated nonlinear analysis to evaluate the structural response of low-rise reinforced concrete residential buildings designed according to outdated seismic code. The results from the performed analyses emphasize the need for selecting suitable reinforced concrete column cross-sections and arranging them properly in plan. When selecting rectangular cross-sections with one relatively small section side, greater attention should be given to the arrangement of the columns in plan in order to provide satisfactory capacity and deformability of the structure in both directions. Even though, the global behaviour of the structure can be optimized by applying these measures, it is doubtful whether this type of columns assures resilience of the structure. Additionally, the capacity of the columns is strictly limited in the up-to-date seismic codes when one needs to follow the “strong column / weak beam” principle. In any case, it is established that the square column sections demonstrated balanced behaviour in both orthogonal directions. The response of the

structure designed with rectangular columns only is somewhat similar in x and y-directions which represents the desired behaviour in seismic design.

The use of more sophisticated, even though simplified, analysis procedure demonstrates the need for application of these techniques when considering highly nonlinear behaviour of the structures. The SPO analysis itself is providing solid information about the performance of the investigated structures. However, the fragility analysis of the same structures contributes by supplying more detailed data about the performance beyond the safety points defined by the codes.

References

- [1] INFRANAT (2019). Increased Resilience of Critical Infrastructure under Natural and Human-induced Hazards (INFRA-NAT), *Deliverable D1.1*, INFRANAT Project, Italy.
- [2] CEN (2005). EN 1998-3:2005. Eurocode 8: Design of structures for earthquake resistance - Part 3: Assessment and retrofitting of buildings, Comité Européen de Normalisation, Brussels.
- [3] Computers and Structures Inc. (2018). CSI PEFORRM-3D- Components and Elements. Version 7.
- [4] Mander J.B., Priestley M.J.N., Park R. (1988). Theoretical stress-strain model for confined concrete, *ASCE Journal of Structural Engineering*, **114** (8): 1804-1826.
- [5] Elghazouli, A. (Ed). (2009). Seismic Design of Buildings to Eurocode 8, 1st Ed., *CRC Press*.
- [6] Haselton C., Whittaker A., Hortacsu A., Baker J., Bray J. & Grant D. (2012). Selecting and scaling earthquake ground motions for performing response-history analyses, *Proceedings of the 15th World Conference on Earthquake Engineering*, Lisbon, Portugal.
- [7] Sullivan, T.J., Saborio-Romano, D., O'Reilly, G.J., Welch D.P., Landi L. (2018). Simplified Pushover Analysis of Moment Resisting Frame Structures, *Journal of Earthquake Engineering*, **25** (4): 621-648.
- [8] O'Reilly G.J., Sullivan T.J. (2018). Quantification of modelling uncertainty in existing Italian RC frames, *Earthquake Engineering & Structural Dynamics*, **47**: 1054-1074.
- [9] FEMA (1997). NEHRP Guidelines for the Seismic Rehabilitation of Buildings. Report No. 273, *Federal Emergency Management Agency*, Washington DC.
- [10] FEMA (2009). FEMA P695: Quantification of Building Seismic Performance Factors. Washington, DC, USA.
- [11] FEMA (2012). FEMA-58-1: seismic performance assessment of buildings volume 1—methodology. *Prepared by ATC for FEMA*, Washington, DC.
- [12] Bentz, E.C., Collins, M.P. (2000). Response 2000. Software program for load-deformation response of reinforced concrete section.
- [13] Cornell C. A., Krawinkler H. (2000). Progress and challenges in seismic performance assessment. *PEER Center News* 3(2): 1–3.
- [14] Vamvatsikos D., Cornell C. A. (2002). Incremental dynamic analysis. *Earthquake Engineering & Structural Dynamics*, **31** (3): 491–514.
- [15] Vamvatsikos D., Cornell C. A. (2006). Direct estimation of the seismic demand and capacity of oscillators with multi-linear static pushovers through IDA. *Earthquake Engineering & Structural Dynamics*, **35**:1097–1117.
- [16] Baltzopoulos, G., Baraschino, R., Iervolino, I. & Vamvatsikos, D. (2017). SPO2FRAG: software for seismic fragility assessment based on static pushover. *Bull Earthquake Eng*, **15**: 4399–4425.
- [17] De Luca F., Vamvatsikos D., Iervolino I. (2013). Near-optimal piecewise linear fits of static pushover capacity curves for equivalent SDOF analysis. *Earthquake Engineering & Structural Dynamics* **42** (4):523–543.